



Seismic behavior of timber-framed structures infilled with dry brick masonry

Aanisa Gani¹ · Jan Mohammad Banday¹ · Durgesh C. Rai²

Received: 5 May 2023 / Accepted: 26 August 2024
© The Author(s), under exclusive licence to Springer Nature B.V. 2024

Abstract

Earthquake-prone regions have seen the resilience of traditional timber-framed masonry construction systems through previous seismic events. The post-earthquake studies show that these building systems have exceptional resilience to seismic activity and can endure multiple seismic events throughout their lifespan. This performance stands out from many contemporary constructions. Although there is a significant amount of evidence regarding the distinct behavior of these structures during earthquakes, there is a limited amount of meaningful quantitative experimental data on their seismic performance. This study showcases the findings of a series of half-scale shake table experiments carried out on a single-room; single-story timber frame filled with dry bond brick masonry. Two half-scale models were created and tested on a shaking table to investigate the seismic performance of timber framed masonry structural systems. One model was left without infill, while the other was infilled with dry bond brick masonry. To analyze the dynamic behavior, both models were exposed to random base excitation. Additionally, the models were tested with gradually increasing ground motion to study their response to seismic activity, following a method known as single ground motion record incremental dynamic analysis. The evaluation focused on the dynamic characteristics, including the assessment of natural frequencies, damping, mode shapes, and stiffness degradation. The stiffness decreased to 43% of the undamaged stiffness in the model with bricks and 62% of the undamaged stiffness in the model without infill. An assessment and evaluation were conducted on the peak acceleration and displacement responses, as well as the global hysteresis response. The acceleration response was significantly higher for the model with brick infill, with an amplification of 300%. In contrast, the model without infill had a lower amplification value of 150%. According to the findings of the study, it is evident that the timber framed structure exhibits a significant level of flexibility and deformability. Additionally, the structure's ability to dissipate energy increased as the peak ground acceleration of the input ground motion increased.

Keywords Dry bond masonry · Seismic tests · Shake table · Timber frame · Incremental dynamic analysis

1 Introduction

Traditional construction systems built with timber frames are becoming increasingly popular in seismically active regions worldwide due to their excellent performance during earthquakes. These construction systems are known for their timber frame filled with various materials, including brick masonry, stone masonry, mud, and wood products. Various construction systems have been identified and named in different regions based on their unique framing system configurations and infill materials. For example, in Portugal, it is known as Pombalino; in Germany as Fachwerk; in France as Colombage; in India and Pakistan as Dhajji-Dewari; in India as Ikra house; in Italy as Casa Baraccata; and in Turkey as Himis and Baghdadi. These distinctions have been documented in multiple studies (Langenbach, *Resisting Earth's Forces: Typologies of Timber Buildings in History* 2018). Several studies have been conducted by various researchers over different years (Rai and Murty 2005; Langenbach 2007; Ali et al. 2012; Gani et al. 2021; Cardoso et al. 2004; Ceccotti et al. 2006, 2004; D'Ayala and Tsai 2008). While previous post-earthquake reconnaissance surveys have documented the exceptional behavior of these structural systems during earthquakes (Kaushik and Jain 2007; Rai and Murty 2005; Rai et al. 2011), there is a lack of research specifically focused on confirming their resilience to earthquakes. Previous studies have attributed the ability of these timber framed construction systems to withstand earthquake shaking to the inherent flexibility of timber framing systems, their strong yet lightweight design, and the use of closely spaced vertical posts to support masonry panels. In addition, the timber joints contribute to the improvement of seismic performance through their ability to dissipate energy, as demonstrated by various studies (Kaushik et al. 2009; Gulkan and Langenbach 2004; Gani et al. 2022, 2021).

Dhajji Dewari (Fig. 1) is one such example of a traditional construction system in the northwest of India that has fared exceptionally well during previous seismic events as well as when compared to popular modern structural systems like unreinforced masonry buildings and reinforced concrete frames with masonry infills. This structural system has been used for many decades, built by the local population using materials and resources readily available in the region, resulting in significant cost savings. The systems do not follow a specific layout or design guidelines. Instead, they are built by the local population using resources that are readily available to withstand earthquakes. It is evident from Fig. 1 that the diagonal elements are randomly positioned in the structure, while the grid of horizontal and vertical elements is consistently present in all three images. The random positioning means, that their position and placement is not consistent in all the structures of same or different typology. It is worth noting that these construction systems have a range of earthquake resilient features. These include carefully designed elevation and plan geometry, minimal and small openings, lightweight materials, flexible connections, and reinforced masonry walls. These structures are mostly of three or four stories, and the walls are mostly single wythe thick. The timber used in these constructions varies from one structure to another, some have been constructed using Poplar (a local type of timber), some from Deodar while some even used well seasoned Willow. As has been highlighted in some studies, the type of timber has minimum effect on the behaviour of such structures under seismic loads (Ali, et al. 2012; Gani et al. 2021). The dynamic performance of such structures is improved by the symmetric plan, which prevents the formation of torsional stresses. Additionally, the simple elevation design ensures that inertia forces generated by earthquakes are efficiently transferred through direct load paths. However, it is worth noting that the presence of diagonal elements results in irregular distribution of stiffness. This



Fig. 1 *Dhajji-Dewari* structures in Kashmir, **a** a hospital building, **b** a government department building, and **c** a residential house

leads to the development of torsional stresses which are resisted by the the flexibility of the timber frame. Furthermore, a significant issue in masonry buildings involves the potential for walls to fail out of plane due to the formation of cracks. By dividing the walls into smaller panels, these timber frame systems effectively prevent out-of-plane failure and confine any potential damage. In addition, the ability of structures to resist earthquakes relies on the energy dissipation characteristics of the system. This is achieved through the flexible timber connections of the timber frame and the predefined planes of failure in the form of the bed joints and head joints of masonry (Kaushik et al. 2009).

The timber framed construction systems represent a traditional building typology, usually non-engineered and developed by local population because of need to survive the earthquakes. This attempt by local population gave rise to development of local seismic cultures. These structures are characterized by a basic timber skeleton infilled with different types of materials. The framing system and the infill material varies from place to place and hence different nomenclature is used in various regions of the world, such as, Pombalino in Portugal, Colombage in France, Half-Timber in Britain, Casa Baraccata in Italy, Fachwerk in Germany, Dhajji-Dewari in India and Pakistan, Ikra houses

in India and Himis and Baghdadi in Turkey as highlighted in various studies (Ceccotti et al. 2004; Cardoso et al. 2004), (Ceccotti et al. Seismic behavior of historic timber-frame buildings in the Italian Dolomites 2006) (Langenbach, From "Opus Craticium" to the "Chicago Frame". earthquake-resistant traditional construction 2007) (D'Ayala and Tsai 2008; Ali et al. 2012) (Langenbach, Resisting Earth's Forces: Typologies of Timber Buildings in History 2018) (Gani, Rai and Banday, Seismic behaviour of Timber framed masonry structures: A Comprehensive review 2021). The different configurations of timber framed masonry structures are shown in Fig. 2. As is evident from Fig. 2 these systems are typically constructed with horizontal and vertical elements, however, in some of the typologies diagonal elements are also used. The growing popularity of these structural systems can be attributed to their utilization of easily accessible materials, cost-effectiveness in construction, good aesthetic appearance, and notably, their commendable capacity for seismic resistance.

Despite the notable behavior observed in previous seismic events, these construction systems have not obtained sufficient attention from the engineering community, and there is a lack of comprehensive studies documenting their performance under seismic loads. The seismic resistance of these traditional timber-framed construction systems has also been established by experimental work on their shear walls (Meireles, et al. 2012; Vasconcelos et al. 2015; Poletti and Vasconcelos 2015; Ahmad et al. 2012; Ceccotti et al. 2004; Aktas, et al. 2014). Over time, researchers have shifted their focus from studying the connections of structural systems to exploring various components such as wall panels, full-scale walls, and scaled models of timber frame structures with different types of infill materials. These studies have contributed to advancing our understanding of these structural systems. There has been a lack of extensive investigation into the behavior of timber frame buildings with brick masonry as an infill under seismic loads.

There is a significant gap in understanding timber framed structures, which is further complicated by the diverse range of materials and construction techniques used. These buildings often lack engineering standards and have unique designs. Therefore, it is crucial to investigate the seismic behavior of timber framed structures to safeguard this valuable architectural tradition.

For this study, a shake table test was conducted on a 50% scaled model of a timber frame house. The model represented a single-room single-story house and was tested with and without infill. The testing was done using the uniaxial earthquake simulation system at IIT Kanpur (Sinha and Rai 2009). The principal objectives of this study are (1) to assess the dynamic characteristics of the timber-framed specimens, (2) to evaluate the acceleration response at different heights of the specimen, and (3) to examine how infills, and openings in infills affect their behaviour under seismic loads. Additionally, it seeks to quantify the level of damage in the specimen by examining variations in fundamental frequency and stiffness as the ground motion increases. To accomplish the aforementioned objectives, the models were subjected to a single record incremental dynamic analysis to comprehensively understand their behavior when subjected to gradually increasing seismic loads (Vamvatsikos et al. 2002). The findings demonstrated a satisfactory performance of the test specimen throughout the entire seismic input. The findings of this study will provide valuable insights for the engineering community, enabling them to confidently implement the construction of timber-framed structures in regions prone to earthquakes. This is particularly important as other commonly used construction methods have not proven effective in withstanding seismic activity in the past.



Bahareque (El Salvador)



Baghdadi (Turkey)



Colombage (France)



Casa Baracatta (Italy)



Dhaji-Dewari (Pakistan)



Dhaji-Dewari (India)



Entramados (Spain)



Fachwerke (Germany)



Gingerbread (Haiti)



Himis (Turkey)



Half-Timbered (Sweden)



Key-Peyi (Haiti)



Pombalino (Portugal)



Quincha (Peru)



Ikra House (India)

Fig. 2 Timber framed structures all over the world

2 Experimental study

2.1 Specimen design, geometry and material properties

A 50% scaled down model of a timber-framed structure was constructed. The structure is made of timber and masonry, and consists of a single room and a single story. It has plan dimensions of 1276×1276 mm and a height of 1246 mm. These dimensions were chosen considering the constraints in the size and capacity of the shake table. The framing elements and diaphragm have been derived from the traditional Dhajji-Dewari construction methodology. However, as shown in Fig. 1, the diagonal elements do not follow a clear pattern, so they are excluded from the specimen. The timber frame for both models is identical, with the only variation being the infill used. Model TF features a bare timber frame, while model TFM features a timber frame that is infilled with dry brick masonry. The TFM model featured three openings: a door in the front wall of the specimen and two windows positioned on two opposite walls of the model. As the door was in the front wall, it was referred to as the front wall (FW), while the wall with the window to the right of the door was called the Right Wall (RW), and the wall with the window to the left of the door was called the Left Wall (LW). The main horizontal beams were connected to the main vertical posts using tenon and mortise type connections, while the secondary members were connected using half lap joints. Figure 3 provides a comprehensive illustration of the timber frame, including the joints used and the orientation of both models on the shake table. As can be seen in the Fig. 3a both the models are symmetric along the plane perpendicular to the front wall, i.e., the wall containing door.

Apart from the wall containing door (front wall), the timber frame was the same for the other three walls of the test specimen. To construct the specimen, we used half scale bricks measuring $120 \times 60 \times 37.5$ mm to infill the walls. The timber frame was made from Indian Sal wood, using six different types of timber elements with varying sectional dimensions. The dimensions of the various framing members utilized in the timber frame are provided in Table 1. The models were constructed in the Structural Engineering laboratory at the Indian Institute of Technology Kanpur.

The test models were constructed directly on the shake table platform to prevent any disruption to the masonry before loading. The test specimen was placed on the shake table using steel angle sections specifically designed to secure the timber frame onto the shake table. The angle sections were positioned on the lower band of the timber frame and securely fastened to the shake table. Given the objective of this study to analyze the dynamic behavior of the model, the assumption was made that the model is ideally connected to the foundation, without considering the effects of the foundation and its connection to the frame.

Since wood shows anisotropic and nonhomogeneous characteristics, it typically exhibits different mechanical characteristics in three planes: axial, transversal, and circumferential. However, wood can be regarded as an orthotropic material because its mechanical characteristics show minimal differences in both the transversal and circumferential planes, ensuring accuracy is not compromised. The material properties of the Sal wood were determined in accordance with the IS 1708 (BIS 1986) and ASTM D143 (ASTM D-143 2014) standards. The properties of the half-scale brick and the Indian Sal wood used in this study are presented in Table 2

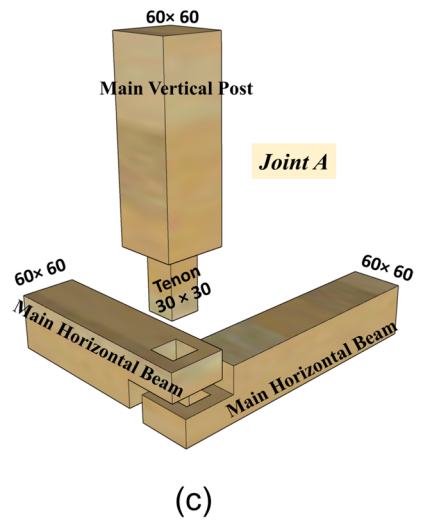
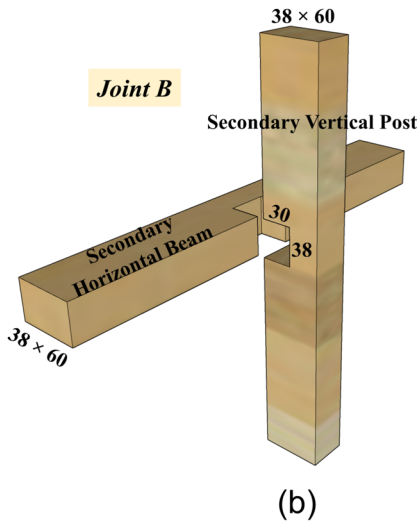
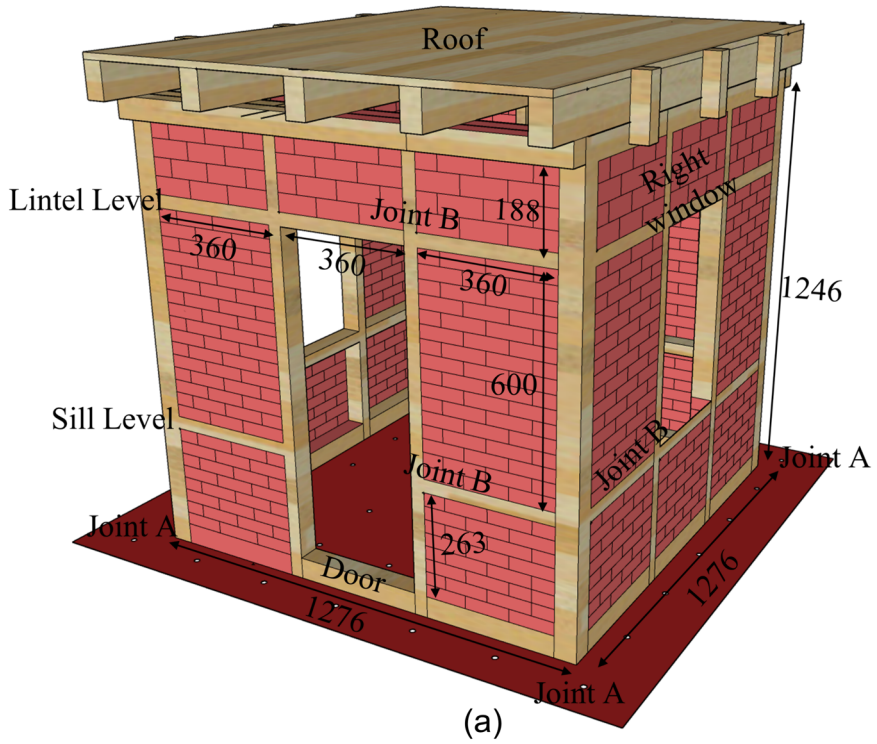


Fig. 3 Details of a the timber frame specimen, b Joint A, and c Joint B

Table 1 Dimension details and number of timber frame members

Member	Cross section	Size (mm) (L×B×H)	Number
Main horizontal beam	Square	1276×60×60	8
Main vertical post	Square	1276×60×60	4
Secondary horizontal beam	Rectangle	1156×60×38	7
Secondary vertical post	Rectangle	1176×60×38	6
Secondary horizontal beam of front wall	Rectangle	360×60×38	2
Secondary vertical post of front wall	Rectangle	1156×60×38	2

Table 2 Mechanical properties of half-scale brick and Indian Sal wood used in this study

Properties	Value
<i>Half scale brick</i>	
Density (kg/m ³) {6}	1792 [0.04]
Weight (kg) {6}	0.495 [0.19]
Compressive strength (MPa) {6}	38.3 [0.22]
<i>Indian sal wood</i>	
Compressive strength parallel to grain (MPa) {6}	50.6 [0.21]
Compressive strength perpendicular to grain (MPa) {6}	39.88 [0.26]
Tensile strength parallel to grain (MPa) {6}	83 [0.15]
Tensile strength perpendicular to grain (MPa) {6}	4.24 [0.19]

{ } = no. of Specimens, [] = coefficient of variation

2.2 Experimental test setup and procedure

Figure 4 displays the experimental setup of both the models (TF and TFM) on the shake table. Steel angle sections securely fastened the timber frame to the shake table platform to ensure stability. To assess the overall seismic performance of the models, sensors were placed at different heights of the walls to measure acceleration and displacement. Figure 5 displays the placement of seventeen accelerometers on different levels of various walls of the model, along with one accelerometer on the shake table platform. In a similar manner, six LVDTs were placed on the two corner posts of the left window wall (LWW) at the sill, lintel, and roof levels. The LVDTs were set up to measure the in-plane displacement of both the walls containing windows. In addition, a total of six wire potentiometers were installed. Three were placed on the rare wall (full infill wall in model TFM) to measure any out-of-plane displacement, while the remaining three were installed on the windows and door, spanning from corner to corner, to monitor any distortion in the openings.

2.2.1 Input signal

The experimental program focused on identifying the dynamic characteristics of the system and investigating the behavior of timber-framed masonry construction systems under seismic loads. To identify the dynamic properties, the specimen underwent white noise excitations. In order to investigate the dynamic behavior of the test specimen, it

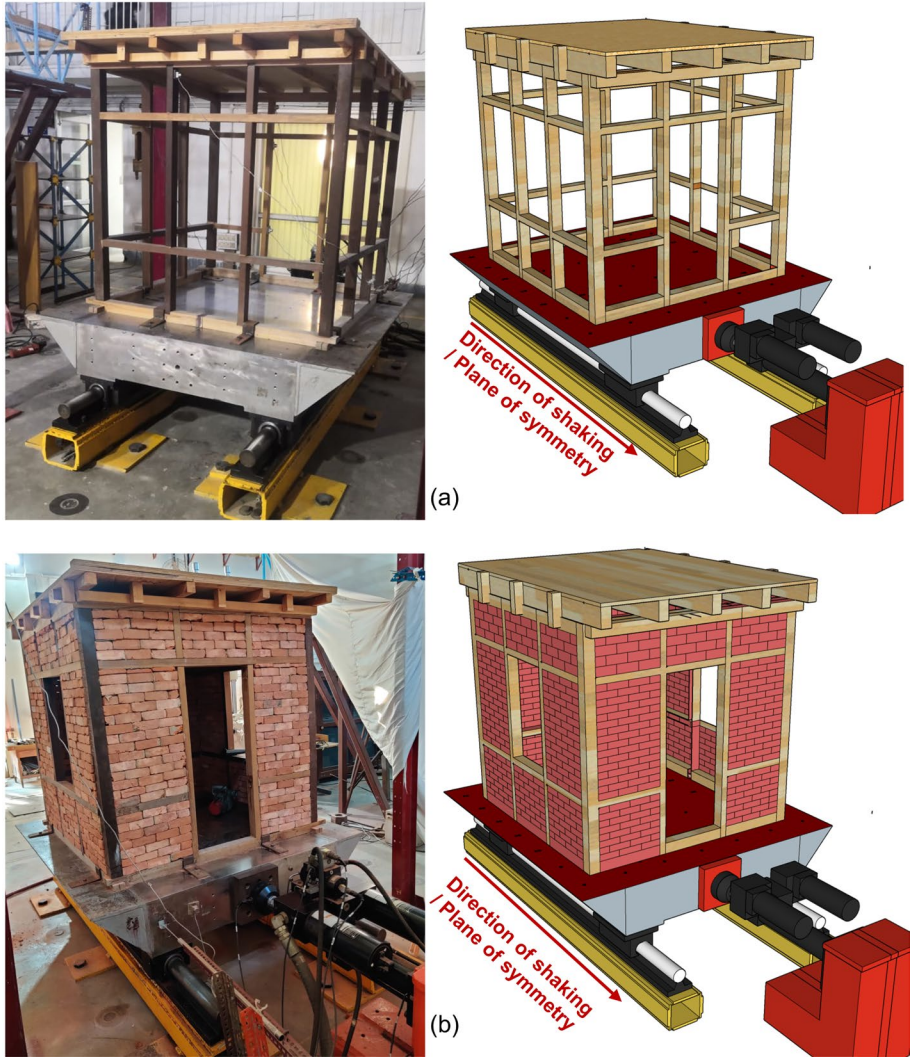


Fig. 4 Test setup of **a** Bare timber frame (TF) model, and **b** Timber frame infilled with dry brick masonry (TFM) model

was exposed to simulated earthquake ground motions that were incrementally increased. One of the classical ground motions was particularly used for the shaking table test. The selected ground motion was the N21E component of the 1952 Kern County earthquake also known as Taft earthquake. It has a peak ground acceleration (PGA) of 0.158 g and a duration of 54.16 s (Fig. 6a). Due to the nature of this study, the time axis of the accelerogram was adjusted to 27 s (Fig. 6b), to meet the requirements of dynamic similitude. Also, the displacement time history used for the test was scaled up according to the similitude relations described in Table 3.

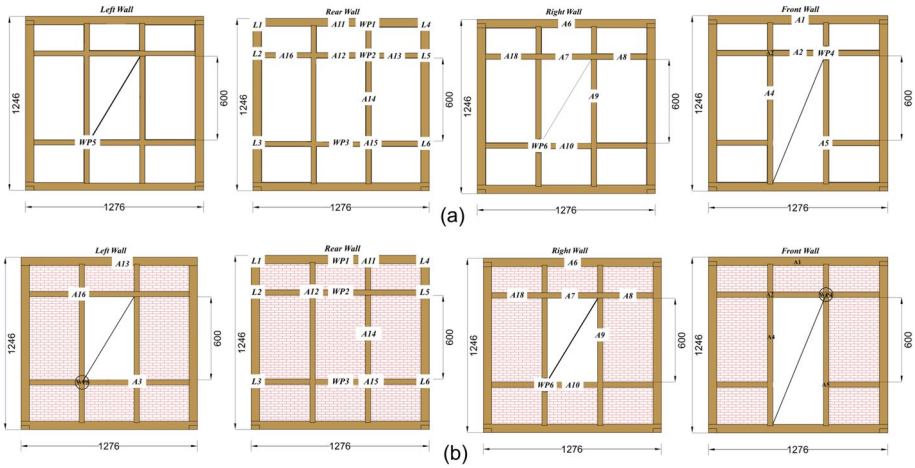


Fig. 5 Instrumentation layout of **a** Bare timber frame (TF) model, and **b** Timber frame infilled with dry brick masonry (TFM) model (A = accelerometer, L = LVDT, WP = wire potentiometer)

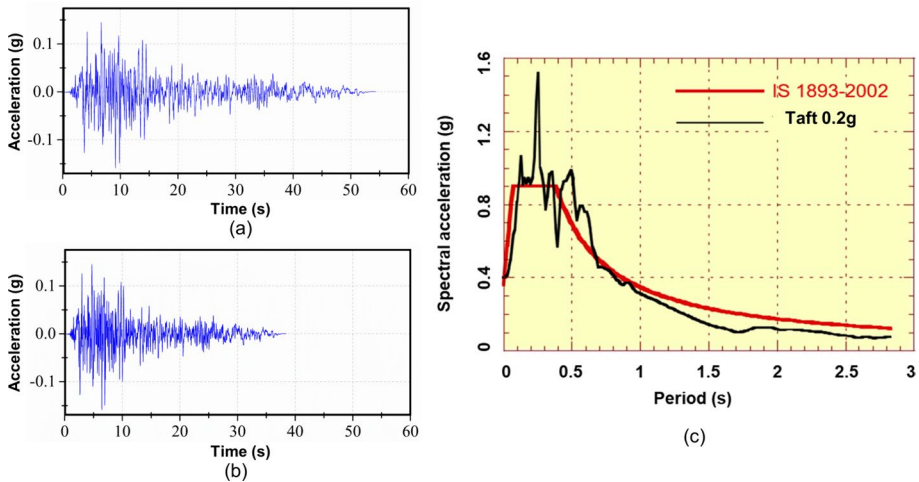


Fig. 6 **a** Original Taft ground motion, **b** Scaled Taft ground motion, **c** Comparison of IBC design response spectrum and original Taft motion upscaled to 0.2 g

Table 3 Similitude requirements

Parameter	Scale factor	Replica model value
Length scale ratio, S_l	l_m/l_p	$1/2$
Modulus ratio, S_E	E_m/E_p	1
Mass density ratio, S	ρ_m/ρ_p	2
Acceleration scale ratio, S_a	a_m/a_p	1
Time scale ratio, S_t	t_m/t_p	$1/\sqrt{2}$
Frequency scale ratio, S	ω_m/ω_p	$\sqrt{2}$

The response spectrum of the Taft ground motion, when scaled to a PGA of 0.20 g, fared reasonably well with the design response spectrum specified in IBC (BIS, 2016) for a design earthquake in Zone V, as shown in Fig. 6c. The shake table tests included using fourteen simulated earthquake ground motions generated by the uniaxial shake table at IIT Kanpur (Sinha and Rai 2009). These fourteen ground motions consist of the PGA of Taft ground motion scaled to fourteen different levels. The levels were categorized based on different PGA values, ranging from 0.05 to 0.70 g. Figure 7 illustrates the loading history schematically. During the experiment, a low-amplitude white noise test was performed to evaluate the variations in stiffness characteristics of the test specimen at different levels of ground motion. By following this loading protocol, it is possible to deduce the reaction of timber-framed masonry buildings to various levels of seismic hazard. This approach is akin to the concept of single-record incremental dynamic analysis (Vamvatsikos et al. 2002).

2.3 Experimental observations under seismic loads

The behavior of the timber-framed structures under seismic loads was analyzed by observing the experimental performance of the bare timber frame specimen and timber frame infilled with dry brick masonry specimen. In addition, the study investigated the dynamic characteristics of both the specimens and the effect of increasing PGA on the behaviour. The presence of window and door openings on the global behavior of such structures was also assessed.

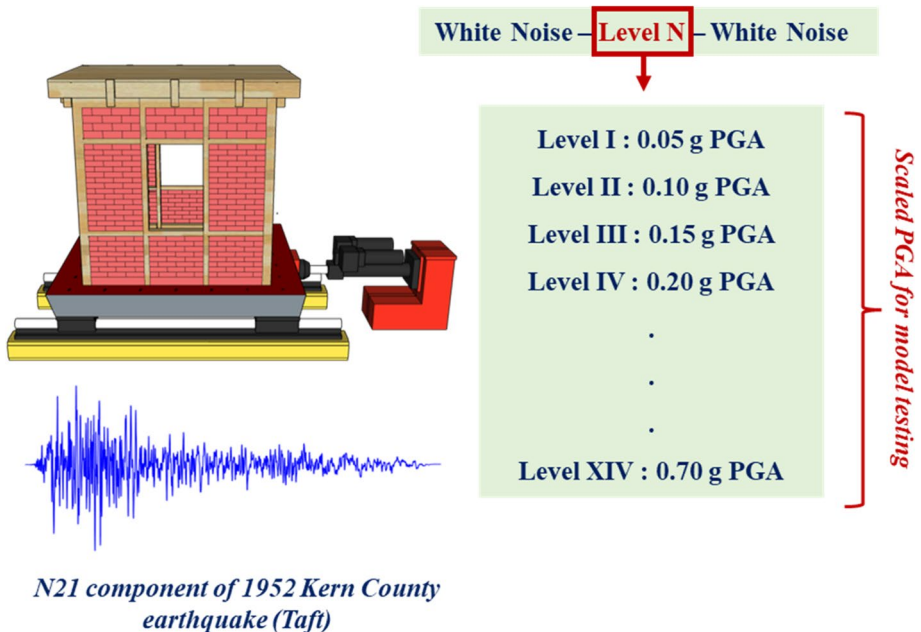


Fig. 7 Loading sequence in accordance with single record incremental dynamic analysis

2.3.1 Effect of dry brick infill

Without infill, timber-framed structures exhibited limited stiffness and lateral force capacity. Also, the tenon connections displayed restricted rotational stiffness, while the column bases functioned as hinges. The displacement capacity of the timber frame before collapse was found to be substantial. The infill increased the lateral resistance and stiffness of the specimen infilled with dry brick masonry, but this comes at the cost of reduced drift capacity. In this study, the focus was on investigating the seismic behaviour of timber frames masonry structures. The impact of using dry brick infill and timber frames as infill walls and how these traditional materials can enhance the lateral capacity and stiffness of the frames were studied. The addition of infill significantly enhanced the lateral capacity and stability of the framed structure.

The stiffness of the infilled timber frame specimen (TFM model) remained 250% higher than the bare timber frame specimen (TF model). The performance of the infill timber frame specimen was significantly enhanced, which can be seen by the resilience of the specimen to increased acceleration amplification of TFM model than the TF model. In fact, the stiffness of the walls surpassed that of the bare frame by over 200 times. Similarly, the maximum drift that could be achieved was significantly reduced by more than 15% compared to the response of the bare frame.

2.3.2 Effect of openings

Openings play a crucial role in the overall structure of a house. It is essential to assess how openings affect the seismic behavior of timber framed structure. Both the specimens (TF and TFM) had two window openings located in the walls subjected to in-plane loads and one door opening in the front wall subjected to out-of-plane loads. The effect of opening was observed in the shake table test of timber framed specimen infilled with dry brick masonry. It was observed that during the test the brick masonry panels displayed relative sliding, i.e., the masonry panels moved individually and the timber frame moved individually. This observation was predominant in the in-plane walls. As the PGA level increased, it was apparent that the top masonry panels of the front wall containing door experienced more damage.

Moreover, the behavior of the wall containing door opening (front wall) stood out significantly from the other walls of the room specimen. However, the comparison of behavior was made between the front wall and the rear wall as both of them are subjected to out-of-plane loads, but the former has an opening while as the rear wall in a full infill wall. During the application of incremental ground motion, as the lateral displacement increased, the doorposts began to lift along with the masonry wall. Subsequently, there was some difficulty with the load transfer between the sill level beam and the main corner posts. This issue arose because of the discontinuity in length of the beam at the sill level, which was caused by the presence of the door opening. It was noted that the load transfer mechanism in front wall varied from the other frames due to the presence of a door.

2.4 Influencing parameters

This section quantifies the impact of different influencing parameters discussed per se on the seismic behavior of the specimens by comparing the dynamic characteristics,

acceleration response, displacement response and the hysteretic behaviour of both the specimens. Also, the comparison of the degradation of stiffness and variation of fundamental frequency between the TF model and the TFM model has been made in the following sections.

2.4.1 Response in the frequency domain

2.4.1.1 Dynamic characteristics of TF model To determine the natural frequencies of the specimen, frequency response functions of the responses derived of the specimen when subjected to white noise excitations were evaluated. Figure 8 displays the Fast Fourier Transform (FFT) of the acceleration time history data obtained from the white noise test done before the seismic test. The specimen exhibited a natural frequency of 2.9–3.6 Hz for the first mode, 4.8–5.16 Hz for the second mode, and 6.8–7.2 Hz for the third mode.

Similarly another key metric the damping ratio regarded as another crucial dynamic characteristic of the examined specimen was also evaluated. The damping ratio is essential in reducing the amplitude of vibrations transmitted to a structure caused by seismic forces. The damping ratios for each individual vibrating mode were found by using frequency domain decomposition (FDD) using MATLAB. This included a thorough analysis of the acceleration time histories that were obtained at various locations on the walls during the white noise test. Figure 9 illustrates the exponential decay curves that accurately represent the three different modes of the material, along with their corresponding damping ratios.

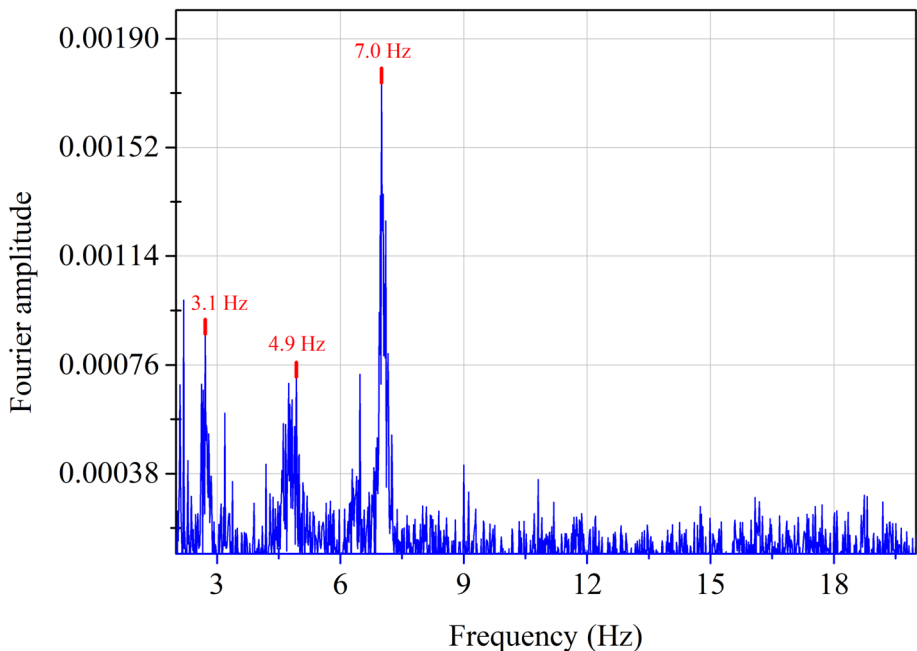


Fig. 8 Fast fourier transform of the acceleration time history highlighting the resonant frequencies of the bare timber frame (TF) specimen

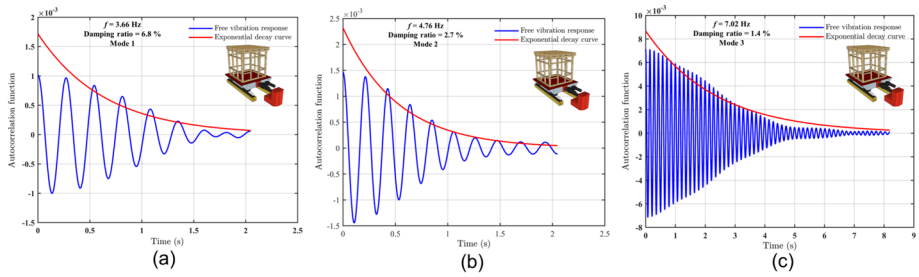


Fig. 9 Exponential decay plots of the timber frame model (TF) **a** Mode1, **b** Mode 2, and **(3)** Mode 3

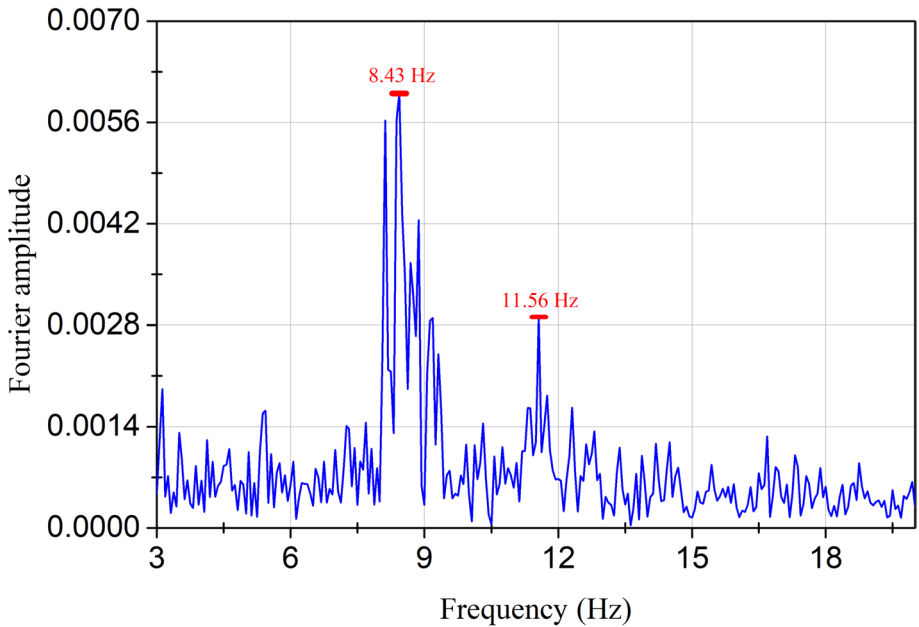


Fig. 10 Fast fourier transform of the acceleration time history highlighting the resonant frequencies of the bare timber frame infilled with masonry (TFM) specimen

2.4.1.2 Dynamic characteristics of TFM model In a similar way the natural frequencies of the timber frame infilled with dry brick infill (TFM model) were determined. Figure 10 displays the Fast Fourier Transform (FFT) of the response acceleration time histories obtained from the white noise tests done prior to the seismic test. The initial undamaged state of the system was characterized by a frequency of 11.58 Hz for t0068e first mode, 18.36 Hz for the second mode and 25.84 Hz for the third mode.

Another important aspect to consider when analyzing the structure is its damping ratio which is essential to decrease the amplitude of vibrations transmitted to a structure when subjected to seismic forces. The damping ratios of the individual vibrating modes identified by FFT have been determined through frequency domain decomposition (FDD) using MATLAB. Figure 11 visually represents the exponential decay curves of the three modes of the specimen along with their respective damping ratios.

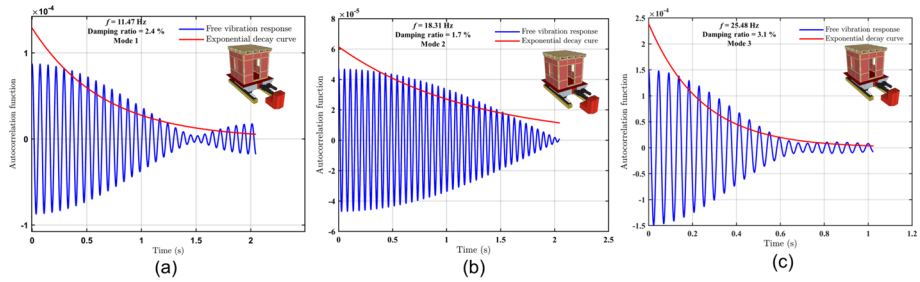


Fig. 11 Exponential decay plots of the timber frame infilled with dry brick masonry model (TFM) **a** Mode 1, **b** Mode 2, and **c** Mode 3

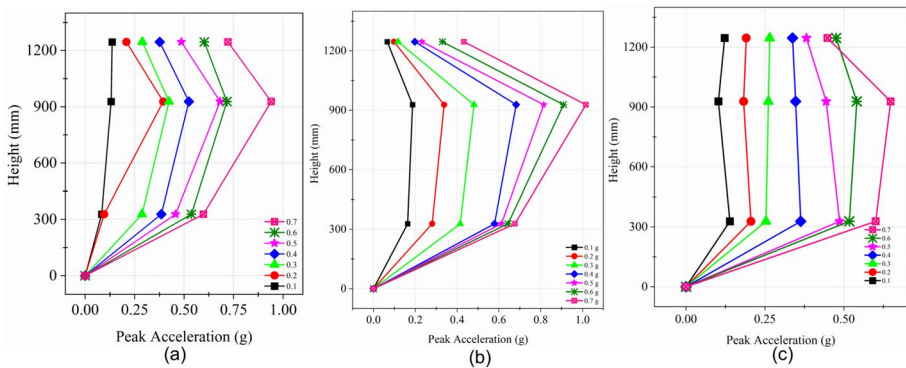


Fig. 12 The acceleration profile of TF model of **a** Rear wall (out-of-plane), **b** Front wall, and **c** Side wall (in-plane)

2.4.2 Response in the time domain

2.4.2.1 Acceleration response of TF model Figure 12 displays the acceleration profile along the height of the different walls of the room specimen at various levels of input ground motion. The acceleration values were obtained from the accelerometers mounted at various levels along the height of the walls. Figure 12c displays the acceleration profile of the right wall which is subjected to in-plane loads. The acceleration profiles of the front wall and the rear wall, both of which are subjected to out-of-plane loads, are shown in Fig. 12a and b. It is evident from the convergence of the profile that the acceleration values decrease at the top in all the profiles. This decrease in acceleration values at the top of the frame is due to the presence of the roof diaphragm which restricts its movement. A significant magnification was observed in the out-of-plane walls, with the rear wall reaching a maximum out-of-plane acceleration of 1 g and the front wall reaching 1.4 g at an input PGA of 0.7 g.

In addition to analyzing the acceleration profiles, the amplification factors, represented by the parameter β , for both the in-plane and out-of-plane walls of the specimen were also evaluated. The parameter β , which is commonly known as the acceleration amplification factor, plays a crucial role in evaluating the seismic response of a structure. Figure 13 displays the changes in acceleration amplification factor for the front wall (Fig. 13a) and right wall (Fig. 13b). From the figure, it is evident that the front wall had a maximum

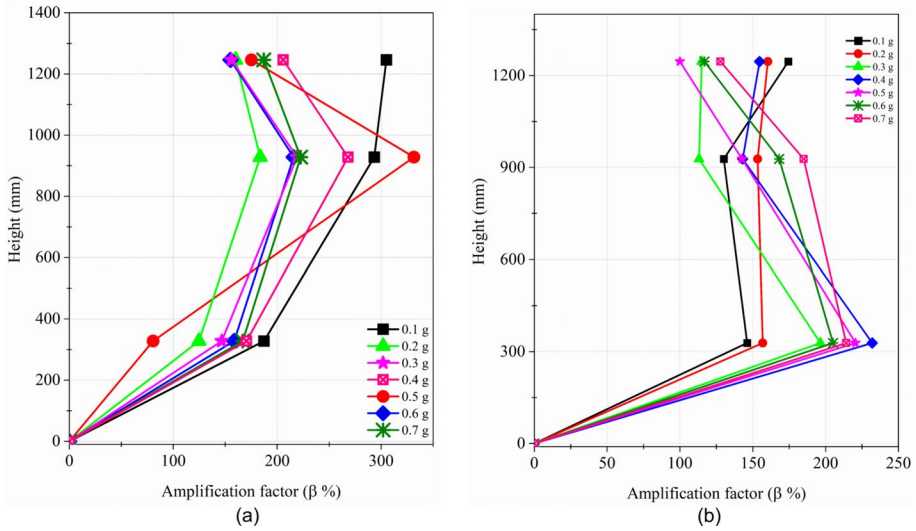


Fig. 13 Variation of acceleration amplification of TF model of **a** Back wall (out-of-plane), **b** Side wall (in-plane) along the height of the specimen

amplification of 350%, while the side wall only reached a maximum amplification of 230%. The difference in behavior is attributed to the front wall being subjected to out-of-plane loads, while the right wall experienced in-plane loads.

2.4.2.2 Acceleration response of TFM model Figure 14 displays the acceleration profile along the height of the different walls of the room specimen when subjected to increasing levels of input ground motion. Figure 14a illustrates the acceleration profile of the out-of-plane wall (the rear wall). Likewise, Fig. 14b displays the acceleration profile of the side wall, the wall subjected to in-plane loads. Upon analyzing all the profiles, it becomes clear that the acceleration values show a consistent decrease towards the top, as observed

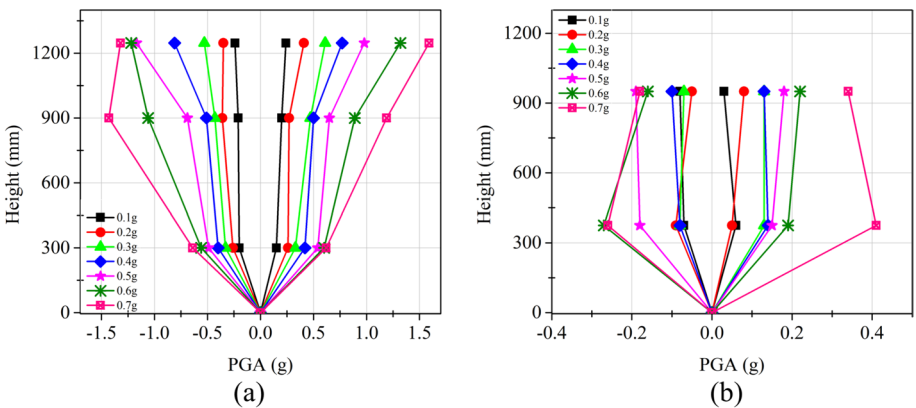


Fig. 14 Acceleration profile of **a** Back wall (out-of-plane), and **b** Side wall (in-plane)

from the convergence of the profile. It is believed that the restricted movement of the frame at the upper part is due to the presence of a roof diaphragm. The out-of-plane acceleration in the wall was measured, reaching a maximum value of 1.7 g for the rear wall. This measurement was obtained at an input peak ground acceleration (PGA) of 0.7 g, suggesting a notable amplification effect.

Furthermore, this study included an assessment of the amplification factors for the in-plane and out-of-plane walls of the specimen. Figure 15 demonstrates the acceleration amplification factor in two distinct walls: the rear wall (Fig. 15a) and the side wall (Fig. 15b). The figure illustrates the observed fluctuations in the acceleration amplification factor at specific locations (sill, lintel, and roof) in these walls. After examining the given data, it is evident that the rear wall (out-of-plane wall) experienced a significant amplification of 290%, as shown in the figure. On the other hand, the maximum amplification on the side wall (in-plane wall) was relatively lower at 100%.

2.4.2.3 Displacement response of TF model The data about the displacement is presented through a displacement profile, specifically emphasizing the in-plane wall and the out-of-plane wall. The profile was recorded using LVDTs placed on two corner posts of the rear wall. In addition, the data for the out-of-plane displacement was acquired using a set of three wire potentiometers, as shown in Fig. 16. As the levels of peak ground acceleration (PGA) gradually increased, a consistent pattern was observed in the displacement responses of the in-plane walls of the specimen. The observed consistent trend demonstrates a significant relationship between the PGA level and the displacement responses of the in-plane walls. Figure 16a shows the absolute in-plane displacement profile of the rear wall, while Fig. 16b displays the absolute out-of-plane displacement profile of the left wall. The measured value for the out-of-plane displacement of the roof of the specimen was found to be approximately 74 mm and that of the in-plane wall was 63 mm.

2.4.2.4 Displacement response of TFM model The displacement data is shown in the form of the displacement of in-plane and out of plane walls, measured using LVDTs and wire potentiometers. The displacement of out-of-plane wall was measured using data obtained from three wire potentiometers positioned on rear wall, as previously illustrated in Fig. 5b.

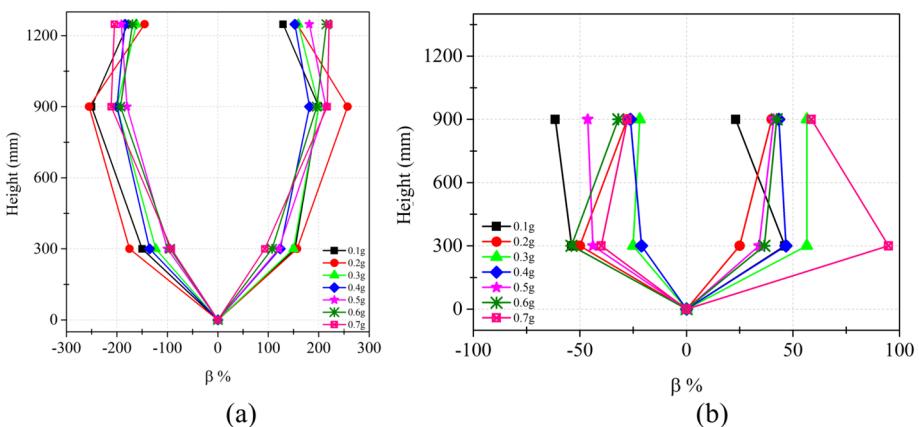


Fig. 15 Variation of acceleration amplification of **a** Back wall (out-of-plane), **b** Side wall (in-plane) along the height of the specimen

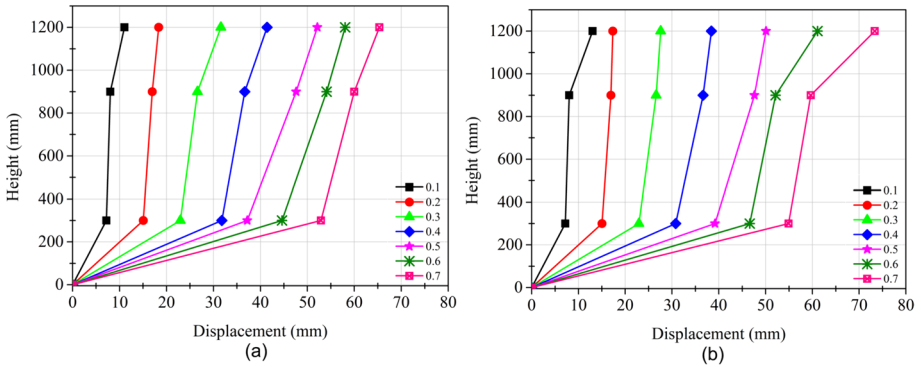


Fig. 16 Variation of displacement of TF model of **a** Side wall (in-plane), and **b** Back wall (out-of-plane), along the height of the specimen

The depicted data points on the graphs represent the absolute displacements that were accurately recorded at the corresponding locations. The displacement responses of the in-plane walls of the specimen were carefully observed and analysed. It was found that these responses consistently followed a discernible pattern as the levels of peak ground acceleration (PGA) were gradually increased. Moreover, it has been observed that the absolute displacement at each level of peak ground acceleration (PGA) demonstrates a proportional increase in line with the corresponding increase in the PGA level of the ground motion. The Fig. 17a shows the absolute in-plane displacement profile of the rear wall (opposite to door wall). Similarly, the Fig. 17b shows the absolute out-of-plane displacement profile of the left wall.

The experimental observation yielded an approximate measurement of 63 mm for the out-of-plane displacement of the roof of the specimen. The direct examination of the walls in the specimen reveals a conspicuous manifestation of displacement, showcasing a persistent upward trend in response to increasing levels of peak ground acceleration (PGA) associated with ground motion. The experimental findings indicate that the model demonstrates a noteworthy maximum story drift of 1/21 when exposed to a peak ground acceleration

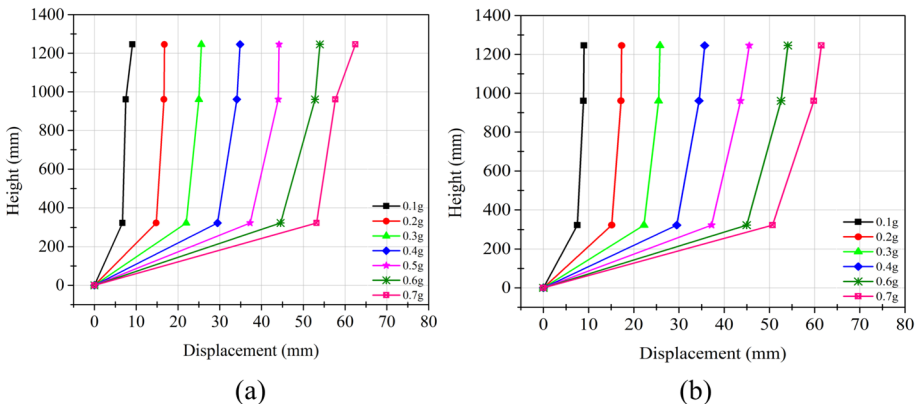


Fig. 17 **a** Out-of-plane displacement profile of left wall, **b** In-plane displacement profile of rear wall

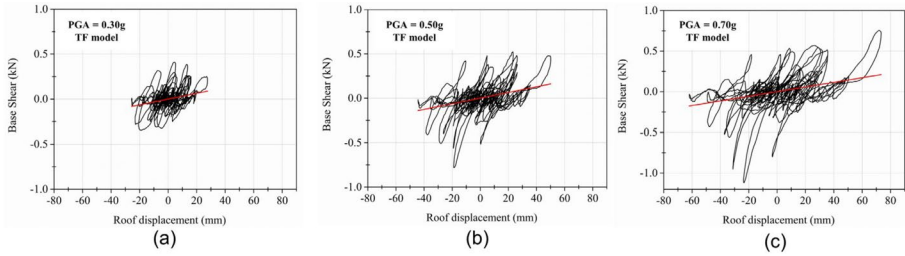


Fig. 18 Hysteresis response of bare timber frame model (TF) at different PGAs

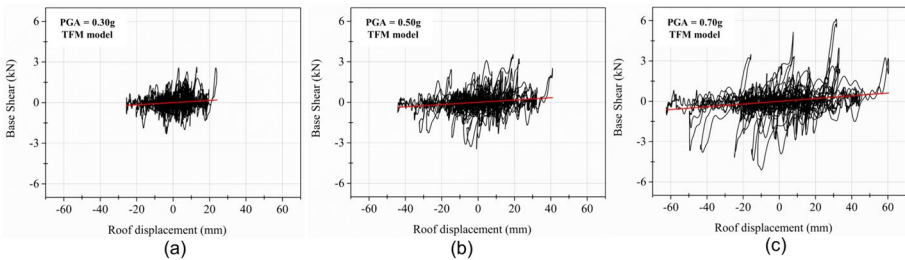


Fig. 19 Hysteresis response of bare timber frame model infilled with dry bond masonry (TFM) at different PGAs

(PGA) level of 0.7 g. According to the technical standard for the maintenance and strengthening of historic timber buildings (Xue and Dan 2018), the mentioned scenario surpasses the prescribed story drift limit of 1/30. Nevertheless, it is important to mention that the structural integrity of the model remained intact, despite the occurrence of minor localized damages in the form of joint loosening. The results of this study suggest that the models exhibited a notable capacity to endure drift limits that surpass the recommended thresholds outlined in the technical standards. Consequently, there exists the potential for additional reinforcement measures to be implemented. The findings of this study highlight the intriguing possibilities of implementing supplementary retrofitting strategies in order to enhance the seismic resilience of historical timber structures.

2.4.2.5 Hysteretic behaviour of TF model Figure 18 displays the hysteresis response of the timber frame model (TF) subjected to the Taft ground motion with increasing PGAs. The base shear of the building was determined by summing the horizontal acceleration measurements and the model mass for a single floor, taking into account the inertia force generated by the models. In the TF model, the hysteresis loop area gradually increased with an increase in the PGA of the input ground motion. This demonstrates that the dissipation capacity is enhanced as the PGA of the input ground motion increases, due to the occurrence of damage in the form of joint loosening in the TF model. However, the energy dissipation capacity of timber frame models is lower since it does not contribute to the overall structure’s stiffness.

2.4.2.6 Hysteretic behaviour of TFM model Similarly, Fig. 19 displays the hysteresis response of the timber frame model infilled with dry brick masonry (TFM) subjected to

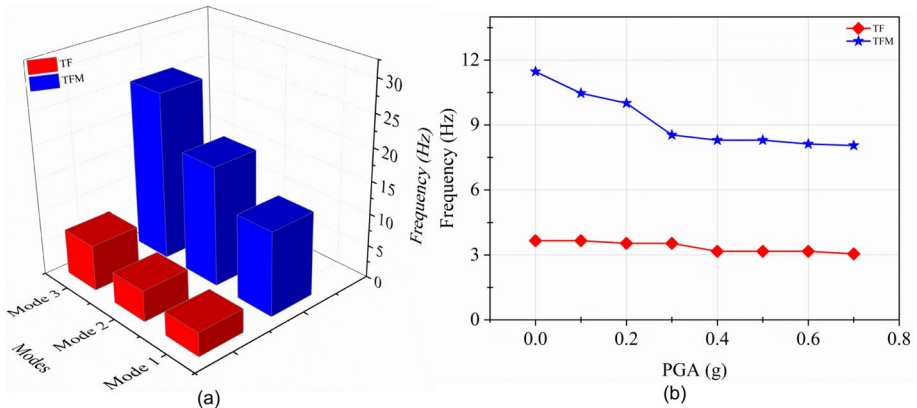


Fig. 20 **a** Natural frequencies of the specimens tested, **b** Change in fundamental frequency of the four specimens

Table 4 Comparison of fundamental frequency of the specimens before and after the application of ground motion

PGA (g)	Fundamental frequency (Hz)	
	TF	TFM
0	3.6	11.47
0.7	3.05	8.05
Percent Reduction	15.28	29.82

the Taft ground motion with increasing PGAs. The figure shows how the energy dissipation was greatly enhanced by incorporating dry bond masonry into the timber frame specimen. This can be explained by the improvement of structural stiffness and also the existence of predetermined failure planes in masonry, especially at the bed joint and the head joint. The presence of predefined failure planes facilitates the dissipation of seismic energy through friction between the two brick units in dry bond masonry. Once more, this emphasizes the importance of using low strength mortar in these types of constructions which serve as predetermined failure planes to effectively disperse energy.

3 Discussion of results

3.1 Response in the frequency domain

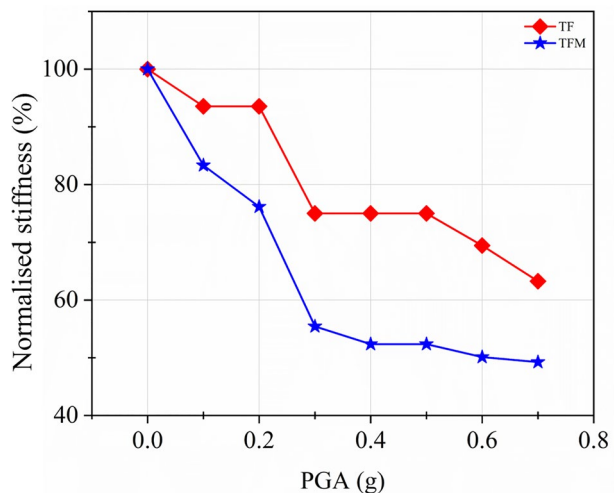
Before and following each ground motion, a white noise test was conducted to identify the changes in the natural vibration frequencies. These tests frequently demonstrated a decline in the natural frequency following each ground motion application to the specimen, suggesting the specimen undergoes a softening process as a result of the accumulated damage it sustains during the test. Figure 20a displays the fundamental natural frequency of the two specimens tested in this study. Also, the variation in the first mode frequencies of the specimens is shown in Fig. 20b. The frequencies at the undamaged

state and at the end of the test can be found in Table 4. The increase in the natural frequencies of TFM specimen, as compared to the TF specimens, can be attributed to the enhanced stiffness in the infilled specimen as well as the increase in mass due to added infill (Aktas and Turer 2016). However, the effect of increase in stiffness was much greater than the effect of increase in mass. Throughout the test, a consistent rate of drop in natural frequency was observed for all specimens.

According to the data in Table 4, the specimens without infill displayed a little variation in natural frequency compared to the specimens with dry brick infill. Specifically, the bare timber frame specimens (TF) experienced a reduction in the range of 15% from its original undamaged state. However, the timber frame specimens infilled with dry brick masonry underwent a significant decrease in the fundamental frequency prior to its failure, of the order of 29% of the undamaged state. This difference in percent reduction can be attributed to the lower stiffness and participating mass of the specimens without infills.

Another aspect important to determine the seismic behaviour of structures is the phenomena of stiffness degradation. It quantifies the accumulated damage in the structures being tested under dynamic loads and thus has significant effect on the reliability and safety of the structures. In this study, the stiffness degradation was evaluated by normalising the stiffness after n th level of ground motion with respect to the undamaged stiffness. The plot of stiffness degradation for the two systems tested for dynamic loads in this study is illustrated in Fig. 6.2. As can be seen in the plot, the stiffness has been normalised and expressed as percentage, with 100% being the undamaged stiffness of all the specimens. The normalised stiffness values have been evaluated at the PGA levels of 0.1, 0.2, 0.3, 0.4, 0.5, 0.6, and 0.7 g. It can be observed that the stiffness degraded steadily after each seismic input and resulted in accumulated damage. It is also apparent that the degradation was severe in the specimens infilled with masonry, i.e., timber frame infilled with masonry (TFM). After the seismic input of 0.7 g PGA, the stiffness degraded to 64% in TF specimen, and 49% in TFM specimen respectively. This stiffness degradation is important to study the post-seismic assessment of the degraded structures (Fig. 21).

Fig. 21 Comparison of stiffness degradation in two systems



3.2 Response in the time domain

The acceleration response of the specimens is expressed as the acceleration profiles of the out-of-plane and in-plane walls with respect to height at different levels of input PGA of the ground motion. Here in this section the variation of acceleration with respect to different PGA levels at the roof of the four specimens is illustrated in Fig. 22a. As can be seen in the figure, the variation of the peak acceleration values was similar in the four specimens, however, the peak acceleration values at 0.7 g PGA varied significantly. The peak acceleration recorded for TF specimen was 1.59 g, and for TFM it was 1.56 g. From the plot, it can be seen that up to an input PGA level of 0.3 g, all the systems had similar acceleration profile, i.e., the variation was similar. It was after 0.3 g input PGA, that the acceleration response changed. This is because of the varied accumulation of damage in the different specimens.

Another aspect of acceleration response evaluated is the acceleration amplification factor. It represents the amplification effects of the specimens to the input seismic excitations. Figure 22b illustrates the variation of amplification factors at the roof level of the out of plane walls of the four specimens. From the figure it can be seen that for initial PGA values the amplification effects are more than the larger PGA values. This can be attributed to the dissipation of energy by the damage initiation in the specimens in terms of friction between the brick units and the between the bricks and the timber frame. This lowest amplification is also seen in the TFM specimen and at a PGA level of 0.7 g. Another reason for this is the period elongation of the specimens as the damage accumulated and which in turn reduced the spectral acceleration of the specimens at the fundamental mode.

Similar to the acceleration response, the displacement response obtained from the LVDTs was expressed as the displacement profiles of the out-of-plane walls. For comparison of the two specimens the displacement time histories at the roof level of the out of plane walls at PGA of 0.7 g of the four specimens is displayed in Fig. 23. The time histories also show the maximum roof displacement of the specimens with 73.10 mm in TF specimen, and 62.21 mm in TFM specimen. The maximum displacement displayed by the bare timber frame (TF) specimen demonstrated the inherent flexibility of the timber frame. It should be, however, noted that even at such large displacements the

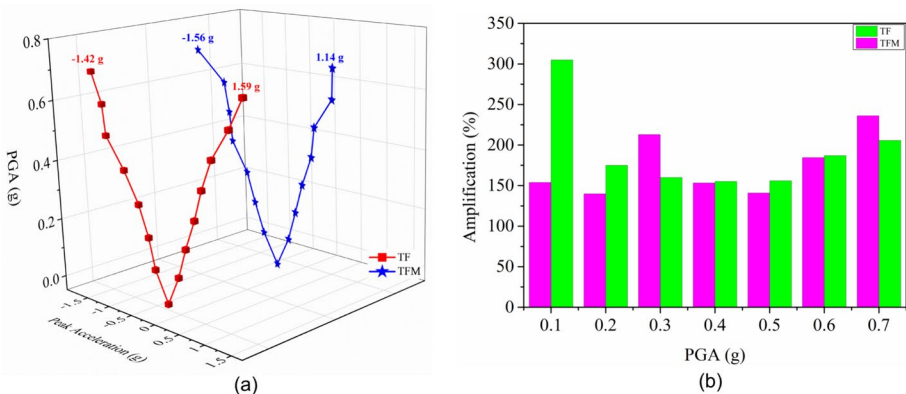


Fig. 22 **a** Comparison of the variation of acceleration at roof level of two specimens at different levels of PGA, and **b** Comparison of acceleration amplification factors of the specimens at roof level

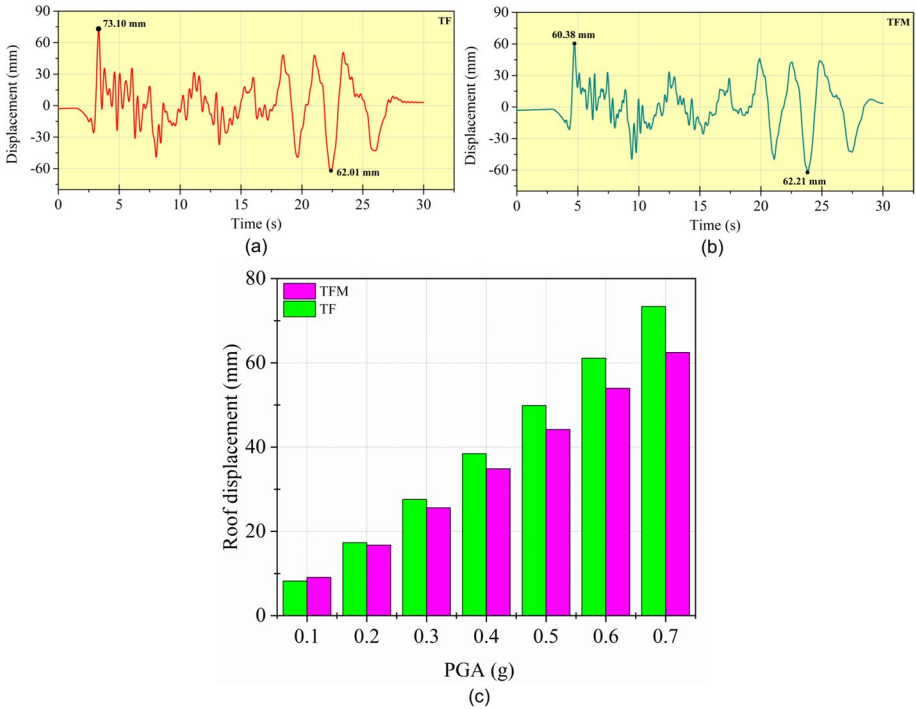


Fig. 23 **a,b** The displacement time histories at roof level at PGA of 0.7 g of TF specimen, and TFM specimen, and **c** Variation of maximum displacements at PGA of 0.7 g at roof level of the four specimens

specimens did not lose the structural integrity. Also, the damage in the specimens was minor and confined to the top masonry panels. This confinement of masonry by timber elements highlights the significance of the timber frame in these structures. The variation of maximum displacement at the roof level with respect to different levels of input PGA of ground motion of the four specimens is shown in Fig. 23c.

Table 5 Story Drift of timber frame specimens with and without infill

PGA (g)	Story drift (displacement at roof/ height of specimen)	
	Model M1 (bare timber frame)	Model M2 (Timber frame infilled with dry bond masonry)
0.1	1/151	1/137
0.2	1/72	1/74
0.3	1/45	1/49
0.4	1/34	1/37
0.5	1/25	1/28
0.6	1/20	1/23
0.7	1/17	1/20

The story drift of two models TF and TFM demonstrates a consistent upward trend as the ground motion PGA increases, as depicted in Table 5. TF model exhibits a maximum story drift of 1/17 at a PGA level of 0.7 g, while the TFM model has a maximum story drift of 1/20. Even though the story drift limits mentioned in the technical standard for maintenance and strengthening of historic timber buildings (Xue and Dan 2018) are exceeded by these limits, both the models did not collapse whereas had a few localised damages.

Furthermore, the comparison of the energy dissipation at varying input PGA of ground motion between TF, TFM specimen is shown in Fig. 24. This figure depicts that by the inclusion of dry bond masonry in the timber frame specimen increased the energy dissipation significantly. From the hysteresis plots it can be inferred that masonry has a significant effect on the energy dissipation capacity of the timber frame structures. This can be attributed to the presence of predefined planes of failure in terms of bed joint and head joint in masonry. These predefined failure planes help to dissipate seismic energy in the form of friction between the two brick units (in the case of dry bond masonry). This again highlights the significance of low strength mortar to be used in such constructions, such that even in the presence of mortar the joints of masonry act as predefined failure planes to dissipate energy.

The experimental study was conducted to evaluate the behaviour of timber framed masonry systems under shake table generated motions. This chapter compared the response

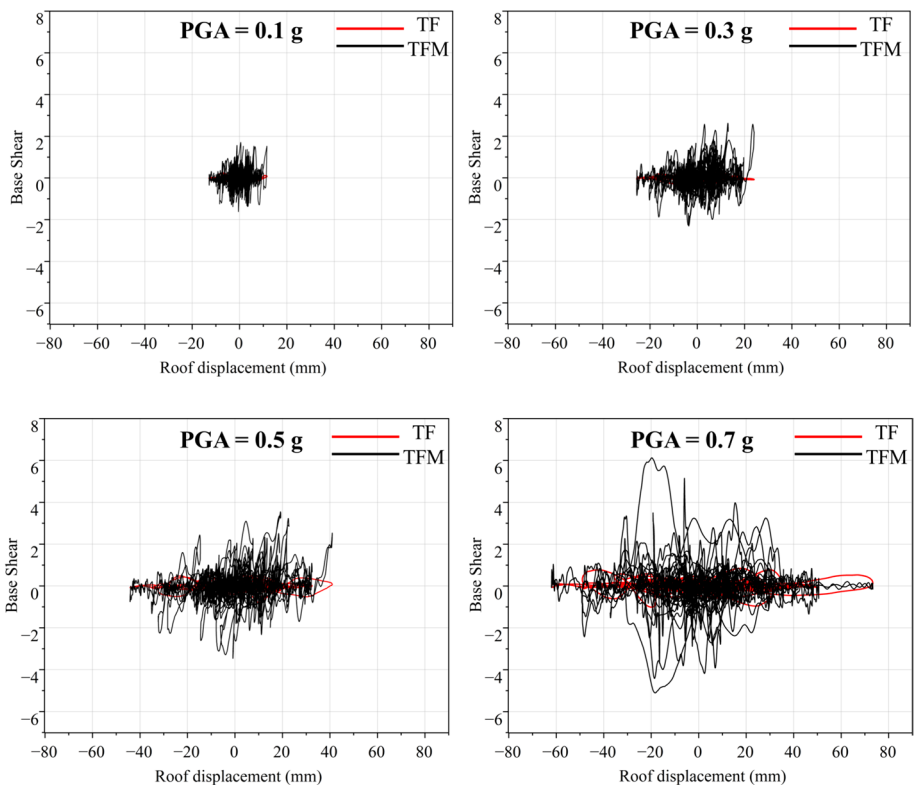


Fig. 24 Hysteresis loops of the timber frame specimen with and without infill at varying PGA of input ground motion

of the two models tested in this study, i.e., TF model, and TFM model. This comparison was done in order to evaluate the significance of all the parameters varied during the testing on the seismic behaviour of timber framed masonry systems. From the comparison it was established that the timber frame is the primary load resisting mechanism system in these structures. However, the infill also has a significant influence on the lateral strength, stiffness, and the overall lateral load behaviour of such structures. The masonry panels in particular reinforce the timber frame by reducing the overall drift response of the structure. Moreover, the flexibility of timber ensures the confinement of masonry and the small movement of individual small panels in response to the lateral loads as described in a study by Gulkan and Langenbach (2004). The brick masonry infill improves the hysteretic behaviour of the timber framed structure. The masonry provides the pre-defined plains of failure along the bed joint and head joint of masonry and therefore increasing the energy dissipation capacity of the system.

4 Summary and conclusions

Shake table tests were conducted on two 1/2-scale models of Dhajji-Dewari structures. The effects of dry brick infill walls on the structural dynamics and seismic behavior of timber-framed structures were studied. The research revealed that the timber-framed structure has a remarkable capacity to withstand seismic loads without sustaining significant damage. This can be attributed to its unique framing system and the presence of flexible joints. The timber frame members and lightweight infill walls (single-wythe brick walls) are important components. One of the main factors contributing to the superior performance of timber-framed structures during severe past earthquakes is the lack of rigid joints in the entire wall-frame system. In addition, the panels used in the house have the advantage of not causing any damage to the surrounding timber frame, even when subjected to significant lateral drifts. This is due to their lightweight nature and the innovative flexible connection they have with the timber frame, which enables the walls to slide within the frame. The wooden frame remained stable even during significant lateral drifts, without any visible damage.

Based on the analysis of the experimental findings, it is evident that the presence of infills has a substantial impact on the lateral strength, stiffness, energy dissipation, and overall lateral load behavior of the timber-framed structure. The inclusion of dry brick infill in the TFM model greatly improved its initial stiffness and energy dissipation compared to the TF model. Based on the experimental investigations carried out, the following conclusions can be drawn:

1. The model with the timber frame infilled with dry bond masonry had a higher natural frequency compared to the model without infill. The higher natural frequency of the former is due to the increased stiffness of the model resulting from the brick infill. The TF model exhibited a natural frequency ranging from 3 to 7.1 Hz, characterized by three prominent modes of vibration. In addition, the TFM model exhibited a natural frequency ranging from 11.5 to 22.4 Hz, showcasing three prominent modes of vibration.
2. As the PGA of the input ground motion increased, both models experienced a gradual accumulation of structural damage. In TF model, damage occurred as joints became loose, while in TFM model, damage involved both loosening of timber joints and falling of bricks. The gradual build-up of structural damage led to a reduction in the stiffness

- of the models, resulting in a decrease in the fundamental frequency. The stiffness of TF model was decreased by 62%, while the stiffness of TFM model was decreased by 43%.
3. The acceleration amplification factors of TF model were 150% and TFM model had a factor of 300%. This demonstrates that the seismic reduction effect was significant. In addition, for PGA values up to 0.4 g, TF model and TFM model exhibited story drifts of 1/34 and 1/37 respectively. These values comfortably meet the applicable standard. It is evident that these structures possess remarkable lateral stability. In addition, for PGA values exceeding 0.4 g, the drift values decreased significantly to 1/17 and 1/20 for TF model and TFM model respectively, without any structural collapse.
 4. When comparing the response of TF model and TFM model, it becomes clear that the presence of dry bond brick infill has a significant impact on the behavior of the timber-framed system. Due to the infill, the lateral stiffness of the system experiences a significant boost, resulting in improved stability.

Acknowledgements The authors are grateful for the fellowship provided by Ministry of Human Resources, India

Author contributions 1. Aanisa Gani: Conceptualization, Methodology, software, formal analysis, investigation, visualization, writing—original draft. 2. Dr. Jan Mohammad Bandy: Supervision, writing—review and editing. 3. Prof. Durgesh C Rai: Conceptualization, validation, resources, supervision, writing—review and editing.

Funding The authors have not disclosed any funding.

Data availability The datasets of the current study are available from the corresponding author on reasonable request.

Declarations

Conflict of interest The authors declare that they have no known competing financial interests or personal relationships that could have appeared to influence the work presented in this paper.

References

- Ahmad N, Ali Q, Umar M (2012) Simplified engineering tools for seismic analysis and design of traditional dhajji-dewari structures. *Bull Earthq Eng* 10:1503–1534. <https://doi.org/10.1007/s10518-012-9364-9>
- Aktas YD, Turer A (2016) Seismic performance evaluation of traditional timber Himiş frames: capacity spectrum method based assessment. *Bull Earthq Eng* 14:3175–3194. <https://doi.org/10.1007/s10518-016-9943-2>
- Aktas YD, Akyuz U, Turer A, Erdil B, Guchan NS (2014) Seismic resistance evaluation of traditional ottoman timber-frame himis houses: frame loadings and material tests. *Earthq Spectra* 30(4):1711–1732. <https://doi.org/10.1193/011412eqs011m>
- Ali Q, Schacher T, Ashraf M, Alam B, Naeem A, Ahmad N, Umar M (2012) In-plane behavior of the dhajji-dewari structural system (wooden braced frame with masonry infill). *Earthq Spectra* 28(3):835–858. <https://doi.org/10.1193/1.4000051>
- ASTM D-143. 2014. Standard Test Methods for Small Clear Specimens of Timber. West Conshohocken, PA
- BIS (1986) Methods of testing of small clear specimens of timber (second Revision). New Delhi, India: IS 1708, Bureau of Indian Standards
- Cardoso, Rafaela, Mario Lopes, and Rita Bento (2004) Earthquake resistant structures of Portugese old 'Pombalino' buildings. In: 13th World Conference on Earthquake Engineering. Vancouver, Canada
- Ceccotti A, Faccio P, Nart M, and Simeone P (2004) Seismic behavior of wood framed buildings in Cadore mountain regioni-Italy. In: 13th World Conference on Earthquake Engineering. Vancouver, BC, Canada

- Ceccotti A, Faccio P, Nart M, Sandhaas C, and Simeone P (2006) Seismic behavior of historic timber-frame buildings in the Italian Dolomites. In: 15th International Symposium Istanbul and Rize. ICOMOS International Wood Committee-15th International Symposium Istanbul and Rize, Turkey
- D'Ayala DF, Tsai PH (2008) Seismic vulnerability of historic Diéh-Dou timber structures in Taiwan. *Eng Struct* 30(8):2101–2113. <https://doi.org/10.1016/j.engstruct.2007.11.007>
- Gani, Aanisa, Durgesh C Rai, and Banday JM (2021) Seismic behaviour of Timber framed masonry structures: A Comprehensive review. In: 17th World Conference of Earthquake Engineering. Sendai: 17th World Conference of Earthquake Engineering, Sendai, Japan
- Gani, Aanisa, Durgesh C Rai, and Jan Mohammad Banday. 2022. "Dynamic Characterization of Timber Frame of Traditional Masonry-filled Construction." *12th National Conference on Earthquake Engineering*. Utah, Salt Lake City
- Gulkan, Polat, and Randolph Langenbach (2004) The earthquake resistance of traditional timber and masonry dwellings in Turkey. In: 13th World Conference on Earthquake Engineering
- Kaushik, Hemant B, and Ravinder Babu KS (2009) Assam-type house
- Kaushik HB, Jain SK (2007) Impact of great December 26, 2004 Sumatra earthquake and tsunami on structures in Port Blair. *J Perform Constr Facil* 21(2):128–142. [https://doi.org/10.1061/\(ASCE\)0887-3828\(2007\)21:2\(12](https://doi.org/10.1061/(ASCE)0887-3828(2007)21:2(12)
- Langenbach R (2007) From “opus craticium” to the “Chicago frame”. Earthquake-resistant traditional construction. *Int J Archit Herit* 1(1):29–59. <https://doi.org/10.1080/15583050601125998>
- Langenbach R (2018) Resisting earth's forces: typologies of timber buildings in history. *Struct Eng Int* 18(2):137–140. <https://doi.org/10.2749/101686608784218806>
- Meireles H, Bento R, Cattari S, Lagomarsino S (2012) A hysteretic model for “frontal” walls in Pombalino buildings. *Bull Earthq Eng* 10(5):1481–1502. <https://doi.org/10.1007/s10518-012-9360-0>
- Poletti E, Vasconcelos G (2015) Seismic behavior of traditional timber frame walls: experimental results on unreinforced walls. *Bull Earthq Eng* 13(3):885–916. <https://doi.org/10.1007/s10518-014-9650-9>
- Rai DC, Murty CVR (2005) Effects of the 2005 Muzaffarabad (Kashmir) earthquake on built environment. *Curr Sci* 90(8):1066–1070
- Rai DC, Mondal G, Singhal V, Parool N, Pradhan T, Mitra K (2011) Reconnaissance report of the M6.9 Sikkim (India–Nepal border) earthquake of 18 September 2011. *Geomat Nat Haz Risk* 3(2):99–111. <https://doi.org/10.1080/19475705.2011.647336>
- Sinha P, Rai DC (2009) Development and performance of single-axis shake table for earthquake simulation. *Curr Sci* 96(12):1611–1620
- Vamvatsikos D, Cornell CA (2002) Incremental dynamic analysis. *Earthq Eng Struct Dyn* 31(3):491–514. <https://doi.org/10.1002/eqe.141>
- Vasconcelos G, Lourenco PB, Poletti E (2015) An overview on the seismic behaviour of timber frame structures. *Hist Earthq-Resist Timber Frames Mediterr Area*. https://doi.org/10.1007/978-3-319-16187-7_10
- Xue J, Dan Xu (2018) Shake table tests on the traditional column-and-tie timber structures. *Eng Struct* 175:847–860. <https://doi.org/10.1016/j.engstruct.2018.08.090>

Publisher's Note Springer Nature remains neutral with regard to jurisdictional claims in published maps and institutional affiliations.

Springer Nature or its licensor (e.g. a society or other partner) holds exclusive rights to this article under a publishing agreement with the author(s) or other rightsholder(s); author self-archiving of the accepted manuscript version of this article is solely governed by the terms of such publishing agreement and applicable law.

Authors and Affiliations

Aanisa Gani¹ · Jan Mohammad Banday¹ · Durgesh C. Rai²

✉ Aanisa Gani
aanisa_17@nitsri.ac.in

Jan Mohammad Banday
jan@nitsri.ac.in

Durgesh C. Rai
dcrai@iitk.ac.in

¹ National Institute of Technology Srinagar, Srinagar 190006, India

² Indian Institute of Technology Kanpur, Kanpur, Uttar Pradesh 208016, India